# Reduction of Stray Loss in Power Transformers Using Horizontal Magnetic Wall Shunts

Masood Moghaddami[1], Arif I. Sarwat[1], and Francisco de Leon[2], *Fellow, IEEE*

[1]Department of Electrical and Computer Engineering, Florida International University, Miami, FL 33174 USA
[2]Department of Electrical and Computer Engineering, Polytechnic Institute, New York University, Brooklyn, NY 11201 USA

**The use of a horizontal arrangement of wall shunts is proposed in this paper as a cost-effective way to reduce the stray losses in power transformers. This paper compares the performance of horizontal wall shunts with the available alternative (vertical shunts). A 3-D finite-element analysis (FEA) is used for the calculation of stray losses in tank walls, and other structural parts. A novel hybrid numerical/analytical method is proposed for the calculation of stray losses inside the magnetic shunts. The proposed method is based on the double Fourier series expansions of the magnetic field distribution at the surface of the shunts, which is determined using 3-D FEA. A 200 MVA power transformer is investigated as a case study where the stray losses are calculated with and without the vertical and horizontal shunts. A parametric FEA is carried out to find the optimal placement of the horizontal shunts on the tank walls. Results show that the proposed horizontal magnetic shunts arrangement are as effective as the conventional vertical shunts in reducing the stray losses while reducing the weight of the shields, therefore providing a cost-effective method for magnetic shielding of the transformer tank walls.**

*Index Terms*—**Finite-element method (FEM), magnetic shielding, power transformer, stray loss, wall shunts.**

## NOMENCLATURE

| | |
|---|---|
| $A$ | Magnetic vector potential (V · s/m). |
| $H$ | Magnetic field (A/m). |
| $B$ | Magnetic flux density (Tesla). |
| $J$ | Eddy-current density (A/m$^2$). |
| $\omega$ | Frequency (rad/s). |
| $\mu$ | Magnetic permeability (H/m). |
| $\nu$ | Magnetic reluctivity (m/H). |
| $\sigma$ | Electrical conductivity (S/m). |
| $P$ | Power loss (W). |

## I. INTRODUCTION

STRAY load losses in transformer tanks and structural parts caused by flux escaping the core play a key role in the transformer overall performance and therefore, reducing these losses is of a great importance for manufacturers. Magnetic wall shunts in power transformers are frequently used to reduce stray losses and eliminate possible hot spots in the tank and structural parts [see Fig. 1(a)]. These types of shields create a low reluctance path for the stray flux and prevent it from reaching the tank. Magnetic shunts are built from laminated steel packets to reduce the losses due to the normal component of the magnetic field to the shunt surface [1].

The design of magnetic shunts is always a great challenge when designing large power transformers. Many studies on the 2-D and 3-D calculations of leakage magnetic field and eddy-current losses in power transformers have been performed [1]–[16]. For the calculation of stray fields in power transformers with magnetic wall shunts, 3-D modeling is needed to accurately compute the effect of different arrangements of magnetic shunts on the stray losses.

Different structures of magnetic shunts in power transformers are studied in [16]–[25], using the finite-element method (FEM) analysis. Horizontal magnetic shunts under the transformer yokes are studied in [20] and [21]. Also, the effect of the lobe-type magnetic shielding on the stray losses of power transformer using the 3-D FEM analysis is studied. In [10], a numerical method based on network approach is presented and it is used in [21] to model the effect of magnetic shunts on transformer stray flux. Many methods are proposed for nonlinear laminated steel modeling and calculation of its stray loss [26]–[36]. The homogenization method has been proposed in [26] and [27] to model the nonlinear laminated steel. In this method, the solution needs to be obtained twice which doubles the calculation time. No study has been performed to investigate the effectiveness of horizontal magnetic wall shunts on transformers stray losses. This type of magnetic shunt diverts the stray flux of the three phases to itself, and thus prevents the flux from entering the tank. Therefore, this technique can effectively reduce the stray losses in large power transformers.

In this paper, a horizontal wall shunt arrangement is proposed and its effectiveness is compared against conventional vertical magnetic wall shunts in reducing the stray losses of power transformers. The investigation is carried out using 3-D finite-element analysis (FEA) using COMSOL Multiphysics. Stray load losses on the tank walls and yoke beams are calculated using surface impedance boundary condition (IBC). Magnetic wall shunts are modeled with nonlinear anisotropic permeability and the corresponding losses are calculated using an analytical method. The presented analytical method uses the magnetic field distribution calculated with 3-D FEM, as boundary condition and Maxwell equations are solved inside the magnetic shunts using the double Fourier series expansion method. Fig. 1(b) shows the 200 MVA

Manuscript received January 20, 2016; revised May 10, 2016; accepted September 9, 2016. Date of publication September 20, 2016; date of current version January 24, 2017. Corresponding author: A. I. Sarwat (e-mail: asarwat@fiu.edu).

Color versions of one or more of the figures in this paper are available online at http://ieeexplore.ieee.org.

Digital Object Identifier 10.1109/TMAG.2016.2611479

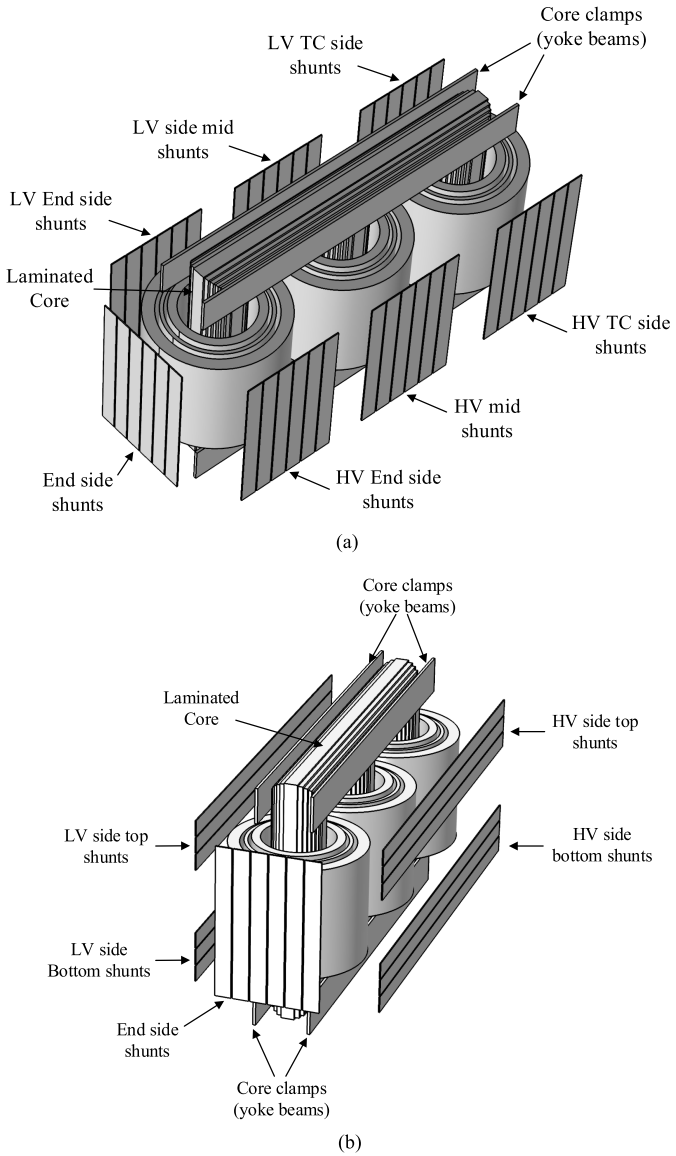


Fig. 1. Three-phase three-legged 200 MVA transformer. (a) Conventional vertical wall shunts. (b) Proposed horizontal wall shunts.

sample transformer with the new proposed horizontal wall shunts.

## II. 3-D Finite-Element Modeling

The 3-D FEM for solving the eddy-current problem uses the quasi-static magnetic vector potential partial differential equation formulation given by

$$\nabla \times (\upsilon(\nabla \times A)) = J_e - j\omega\sigma A. \tag{1}$$

Three-phase full load current excitation is applied to windings. Since the distance between the tank walls and the outer windings is not equal in all directions, no symmetry boundary condition is applied to the 3-D model of the transformer to maximize the accuracy of the analysis.

### A. Impedance Boundary Condition

At the boundaries where the magnetic field penetrates only a short distance into the boundary, the IBC is used for approximating the magnetic field penetration into the boundary. The IBC can be used to model a bounded domain as an unbounded region and is a valid approximation if the skin depth is small compared with the size of the conductor. The penetration depth $\delta$ is measured using the following equation:

$$\delta = \sqrt{\frac{2}{\omega\mu\sigma}}. \tag{2}$$

The IBC boundary condition, which is a combination of the Dirichlet and Neumann boundary conditions, proposes a relationship between the value of magnetic vector potential $A$ and its normal derivative at the boundary. This boundary condition can be written as the following equation:

$$\frac{\partial A}{\partial n} + cA = 0 \tag{3}$$

where $c$ is a constant determined by the permeability and conductivity of the boundary material. Since in power transformers, tank walls and yoke beams are made of iron and the penetration depth at 60 Hz for iron is less than 1 mm, in the 3-D FEM model of the transformer, IBC is applied to the interior boundaries of the tank walls and the exterior boundaries of the yoke beams.

### B. Magnetic Shunt Modeling

Magnetic shunts are constructed using laminated steel and therefore should be modeled with nonlinear anisotropic permeability. The magnetization characteristic of M-5 steel (shown in Fig. 3) is used for modeling the nonlinearities of the shunts. The conductivity of the shunts is set to zero in the FEM model, and then, the eddy-current losses are calculated with the analytical method described in Section III.

## III. Magnetic Shunt Loss Calculation

The losses in the magnetic wall shunts can be calculated using a series expansion of eddy-current loss based on the 2-D spatial harmonics of current density inside a magnetic wall shunt. This series can be expressed as follows:

$$P = \sum_{m=1}^{\infty}\sum_{n=1}^{\infty} P_{mn} \tag{4}$$

where $P_{mn}$ is the eddy-current loss due to the spatial current density harmonics. The current density harmonics in the magnetic shunt sheets can be calculated based on an analytical approach provided that the magnetic field distribution on the magnetic shunts surface is known. The analytical solution can be obtained by solving the quasi-static field equations, which are expressed as follows [2]:

$$\nabla^2 H = j\omega\mu\sigma H \tag{5}$$

$$\nabla \cdot H = 0 \tag{6}$$

$$J = \nabla \times H. \tag{7}$$

Fig. 3 shows a laminated magnetic shunt with dimensions of $W \times 2L \times d$. It is assumed that the spatial distribution of the normal component of the magnetic field ($H_z$) on the surface $z = 0$ could be written as a double Fourier series expansion as

$$H_{z0}(x, y) = \sum_{m=1}^{\infty}\sum_{n=1}^{\infty} H_{mn} \cos\left(\frac{m\pi x}{W}\right) \sin\left(\frac{n\pi y}{L}\right) \tag{8}$$

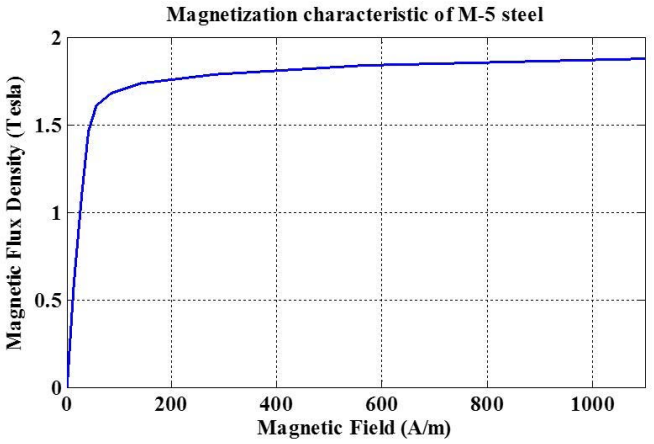


Fig. 2. Magnetization curve of the M-5 steel.

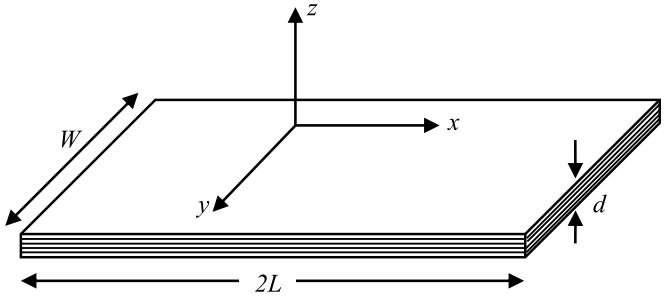


Fig. 3. Laminated magnetic shunt with dimensions of $W \times 2L \times d$.

where $H_{mn}$ are the double Fourier series coefficients, which can be calculated as follows:

$$H_{mn} = \frac{2}{WL}\int_0^W \int_{-L}^{L} H_{z0}(x, y)\cos\left(\frac{m\pi x}{W}\right)\sin\left(\frac{n\pi y}{L}\right). \quad (9)$$

For the calculation of eddy-current loss of the magnetic shunt, first, the loss corresponding to each spatial harmonic is calculated, and then, the superposition is applied in order to calculate the total shunt loss. The spatial harmonic component of (8) could be written as

$$H_{z0}(x, y) = H_{mn}\cos\left(\frac{m\pi x}{W}\right)\sin\left(\frac{n\pi y}{L}\right). \quad (10)$$

This equation can be used as a boundary condition for (5)–(7) in order to calculate magnetic field inside the shunt. By expanding (5) in the direction of the $z$-axis, the following equation is derived:

$$\frac{\partial^2 H_z}{\partial x^2} + \frac{\partial^2 H_z}{\partial y^2} + \frac{\partial^2 H_z}{\partial z^2} = j\omega\mu\sigma H_z. \quad (11)$$

According to (10) and (11), $H_z$ can be written as follows:

$$H_z = H_{mn}e^{\beta z}\cos\left(\frac{m\pi x}{W}\right)\sin\left(\frac{n\pi y}{L}\right)$$
$$\beta^2 = j\omega\mu\sigma + \left(\frac{n\pi}{L}\right)^2 + \left(\frac{m\pi}{W}\right)^2 \quad (12)$$

where the permeability of $\mu$ is determined based on the magnetic flux density in each wall shunt, which is computed by the 3-D FEA, as well as the magnetization characteristic of the M-5 steel, which is shown in Fig. 2.

Using (6) and (12), the following equation can be derived:

$$\frac{\partial H_x}{\partial x} + \frac{\partial H_y}{\partial y} + \frac{\partial H_z}{\partial z} = 0$$
$$\frac{\partial H_x}{\partial x} + \frac{\partial H_y}{\partial y} = -H_{mn}\beta e^{\beta z}\cos\left(\frac{m\pi x}{W}\right)\sin\left(\frac{n\pi y}{L}\right). \quad (13)$$

Since the magnetic shunts are laminated, current cannot flow in the direction of the $z$-axis, based on (7) it can be expressed as the following equation:

$$J_z = \frac{\partial H_y}{\partial x} - \frac{\partial H_x}{\partial y} = 0. \quad (14)$$

It is assumed that the solution for $H_x$ and $H_y$ can be written as follows:

$$H_x = K_1 H_{mn}e^{\beta z}\sin\left(\frac{m\pi x}{W}\right)\sin\left(\frac{n\pi y}{L}\right)$$
$$H_y = K_2 H_{mn}e^{\beta z}\cos\left(\frac{m\pi x}{W}\right)\cos\left(\frac{n\pi y}{L}\right) \quad (15)$$

where $K_1$ and $K_2$ are unknown constants which can be calculated using (13) and (14) as follows:

$$K_1 = -\frac{H_{mn}L^2 mW\beta}{m^2\pi L^2 + n^2\pi W^2}$$
$$K_2 = \frac{H_{mn}LnW^2\beta}{m^2\pi L^2 + n^2\pi W^2}. \quad (16)$$

Thus, the final solution of $H_x$ and $H_y$ can be expressed as following set of equations:

$$H_x = -\frac{H_{mn}L^2 mW\beta}{m^2\pi L^2 + n^2\pi W^2}e^{\beta z}H_{mn}e^{\beta z}\sin\left(\frac{m\pi x}{W}\right)\sin\left(\frac{n\pi y}{L}\right)$$
$$H_y = \frac{H_{mn}LnW^2\beta}{m^2\pi L^2 + n^2\pi W^2}e^{\beta z}H_{mn}e^{\beta z}\cos\left(\frac{m\pi x}{W}\right)\cos\left(\frac{n\pi y}{L}\right). \quad (17)$$

Using solutions for magnetic field components (17) current density distribution can be calculated using (7) and the following equations can be deducted for the current density components $J_x$ and $J_y$:

$$J_x = \frac{nH_{mn}[n^2\pi^2W^2 + L^2(m^2\pi^2 + W^2\beta^2)]}{L\pi(L^2m^2 + n^2W^2)} \times e^{\beta z}\cos\left(\frac{m\pi x}{W}\right)\cos\left(\frac{n\pi y}{L}\right)$$
$$J_y = \frac{mH_{mn}[n^2\pi^2W^2 + L^2(m^2\pi^2 + W^2\beta^2)]}{W\pi(L^2m^2 + n^2W^2)} \times e^{\beta z}\sin\left(\frac{m\pi x}{W}\right)\sin\left(\frac{n\pi y}{L}\right). \quad (18)$$

Using (18), spatial distribution of eddy-current loss density can be expressed as follows:

$$P_v = \frac{J.J^*}{2\sigma} = \frac{H_{mn}^2L^2W^2\mu^2\sigma\omega^2}{2\pi^2(L^2m^2 + n^2W^2)^2}e^{-2\mathrm{Real}(\beta)} \times\left[n^2W^2\cos^2\left(\frac{m\pi x}{W}\right)\cos^2\left(\frac{n\pi y}{L}\right) + m^2L^2\sin^2\left(\frac{m\pi x}{W}\right)\sin^2\left(\frac{n\pi y}{L}\right)\right]. \quad (19)$$

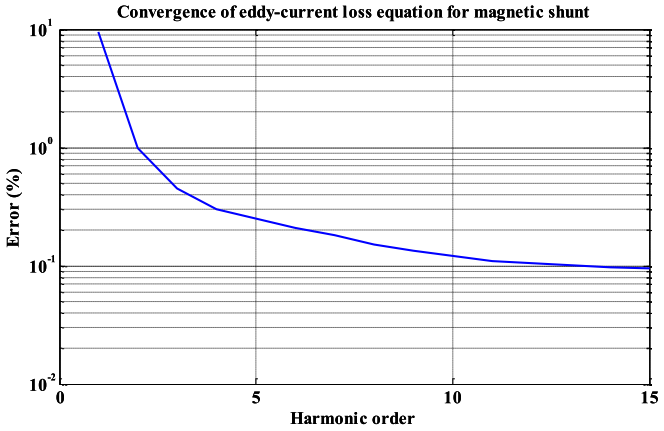


Fig. 4. Convergence of the eddy-current loss series expansion presented in (4) for the case study transformer.

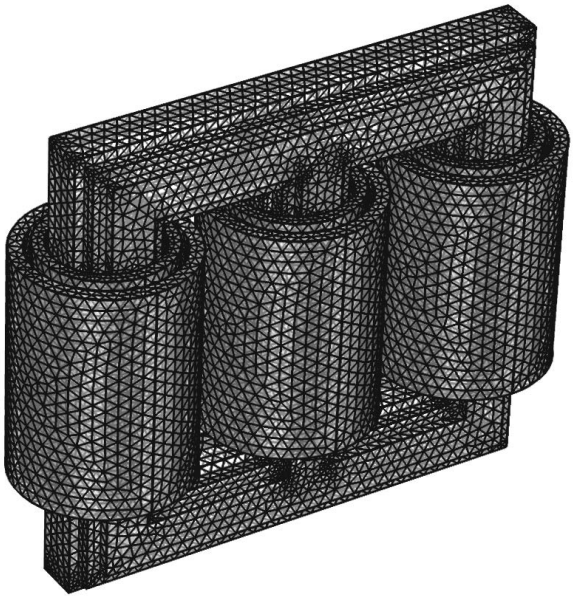

Fig. 5. Mesh of the case study transformer model without wall shunts consisting of 817 155 elements.

And the solution for the calculation of loss due to the normal component of magnetic field at $z = 0$ surface can be derived as follows:

$$P_{mn} = \int_{-\infty}^{0}\int_{-L}^{L}\int_{-W/2}^{W/2} P_v dx dy dz = \frac{H_{mn}^2 L^3 W^3 \mu^2 \sigma \omega^2}{8\pi^2 (L^2 m^2 + n^2 W^2)\text{Real}(\beta)}. \quad (20)$$

Using (4) and (20), the total eddy-current loss of the magnetic shunt shown in Fig. 3 can be written as follows:

$$P = \frac{\mu^2 \sigma \omega^2}{8\pi^2} \sum_{m=1}^{\infty}\sum_{n=1}^{\infty} \frac{L^3 W^3 H_{mn}^2}{(L^2 m^2 + n^2 W^2)\text{Real}(\beta)}. \quad (21)$$

Equation (21) presents the series expansion of the eddy-current losses of a magnetic shunt based on the Fourier series expansion of magnetic field on its surface.

For the calculation of magnetic shunts losses based on the presented analytical method, magnetic field distribution on the shunts surface is calculated with 3-D FEA using COMSOL Multiphysics. The calculated magnetic field distribution is exported into MATLAB and the double Fourier series coefficients of (8) are calculated using (21), and thus, the total loss of the magnetic shunt can be obtained. Fig. 4 shows the convergence of (21) for a sample vertical magnetic shunt. Fig. 4 shows that by expanding this equation up to the 15th component in both the $x$ and $y$ axes, the convergence error would be less than 0.1%.

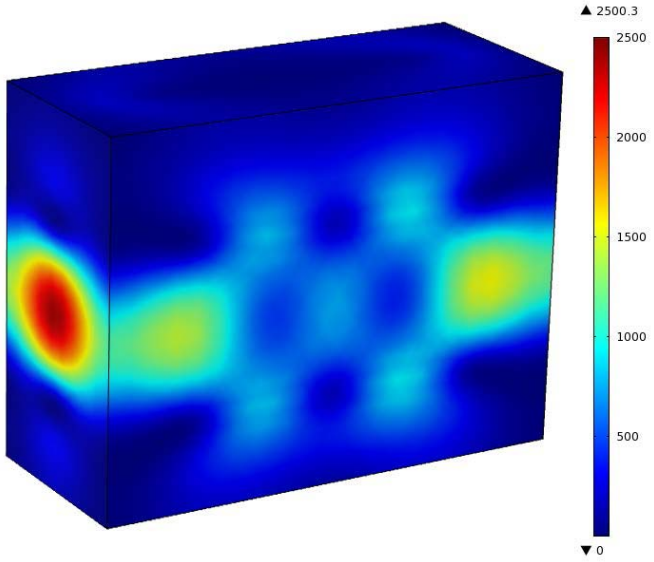


Fig. 6. Eddy-current loss density (W/m$^2$) distribution on transformers tank without any magnetic shunts.

TABLE I
COMPARISON OF STRAY LOSSES IN DIFFERENT WALL SHUNT ARRANGEMENTS

| Parameter | Without Shunts | Vertical Shunts | Horizontal Shunts |
|---|---|---|---|
| Tank Loss ($W$) | 58993 | 5981 | 5458 |
| Yoke-Beam Loss ($W$) | 17893 | 5439 | 5368 |
| Shunt Loss ($W$) | – | 1740 | 2236 |
| Total Loss ($W$) | 76886 | 13160 | 13062 |
| Total Loss Reduction (%) | – | 82.88 | 83.01 |
| Total Shunt Weight ($kg$) | – | 2671 | 2009 |

## IV. Results and Discussion

In this section, the 200 MVA transformer shown in Fig. 1(a) and (b) is considered as a case study to compute the stray losses of tank, yoke beams, and magnetic shunts for three scenarios: transformer without magnetic shunts, transformer with the vertical magnetic shunts, and transformer with the horizontal magnetic shunts. In Sections IV-A–IV-C, the results are presented and comparisons are made.

### A. Transformer Without Magnetic Shunts

In this case, the transformer carrying full load is considered and the stray losses in tank walls and yoke beams are calculated. The mesh of the 3-D model consists of 817 155 elements and is shown in Fig. 5. The total stray loss is 76.89 kW. The results are presented in Table I. Fig. 6 shows the loss density distribution in W/m$^2$ on tank walls. As it can be seen the loss density on the tank walls in the area between adjacent

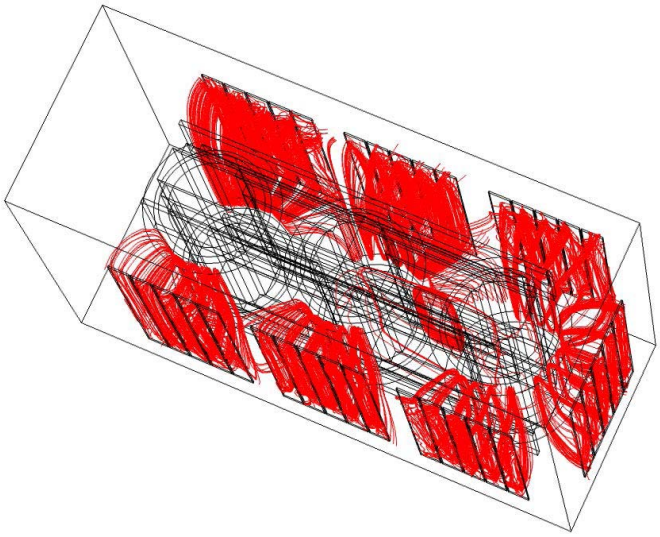

Fig. 7. Magnetic leakage flux lines diverted by the vertical magnetic shunts.

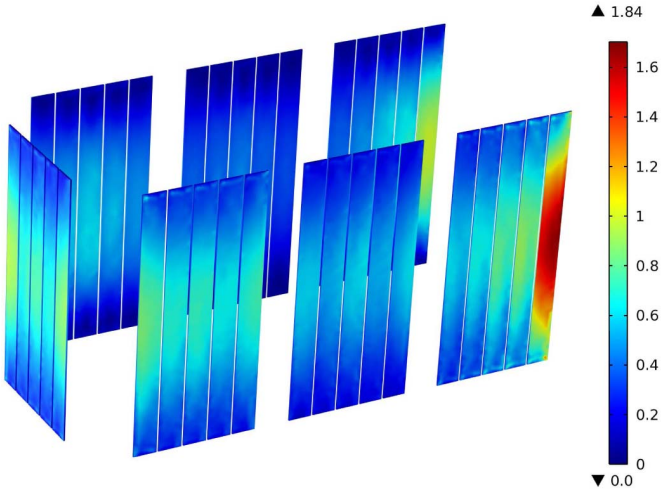


Fig. 8. Magnetic flux distribution (Tesla) in the vertical magnetic shunts.

windings is lower than the other areas of the tank walls, which is the cause of leakage flux cancelation of adjacent windings. On the other hand, the maximum loss density occurs on the side tank wall. Also, the loss density distribution has a completely different pattern on main tank walls compared with side tank wall.

### *B. Transformer With Vertical Magnetic Shunts*

In this case, vertical magnetic wall shunts are used to reduce stray losses. In front of windings on each limb of the transformer, five laminated shunts are placed on the tank walls. Shunts are not placed on tap-changer side of the tank due to its low stray loss. The mesh of the 3-D model consists of 2 182 302 elements. The calculation results are presented in Table I. Fig. 7 shows the magnetic leakage flux lines. Fig. 7 shows that the flux lines are completely diverted by magnetic shunts and as a result, the eddy-current losses in the tank walls and the yoke beams are reduced 82.88% when compared with the transformer without wall shunts. The magnetic flux distribution in the vertical magnetic shunts is shown in Fig. 8.

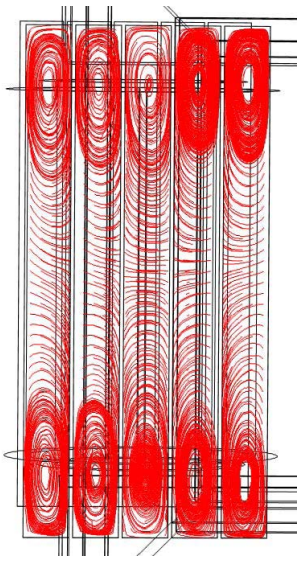

Fig. 9. Induced current density streamlines on vertical shunt packets surfaces.

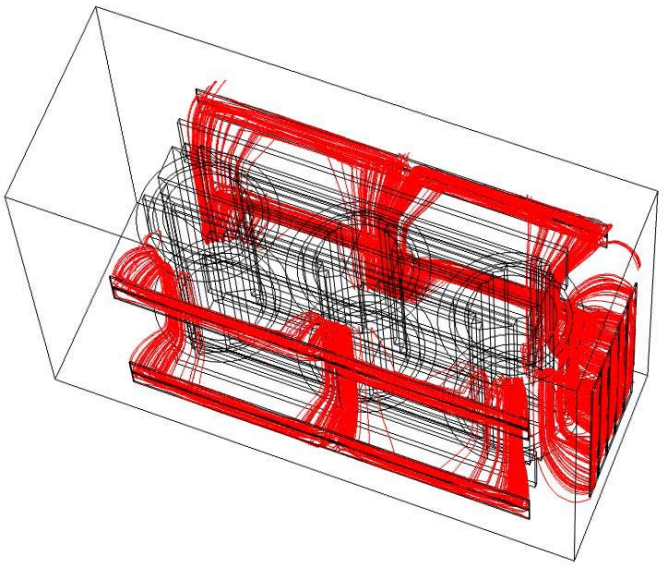

Fig. 10. Magnetic leakage flux lines diverted by the horizontal magnetic shunts.

Fig. 8 shows that the flux is not distributed uniformly in the shunt packets and it is higher on the side shunt packets. Also, it can be seen that wall shunts in the center phase have a lower flux density. Therefore, the thickness of these shunts can be reduced. Fig. 9 shows the induced current density streamlines on vertical shunt packet surfaces of one phase.

### *C. Transformer With Horizontal Magnetic Shunts*

In this case, the horizontal and vertical magnetic wall shunts are used to reduce stray losses. In front of the three phases of the transformer, six horizontal laminated shunts are placed on the tank walls (three shunts at top and three shunts at bottom). The mesh of the 3-D model consists of 1 853 022 elements. The calculation results are presented in Table I. Fig. 10 shows the magnetic leakage flux lines. Fig. 10 shows that the flux lines are completely diverted by the horizontal

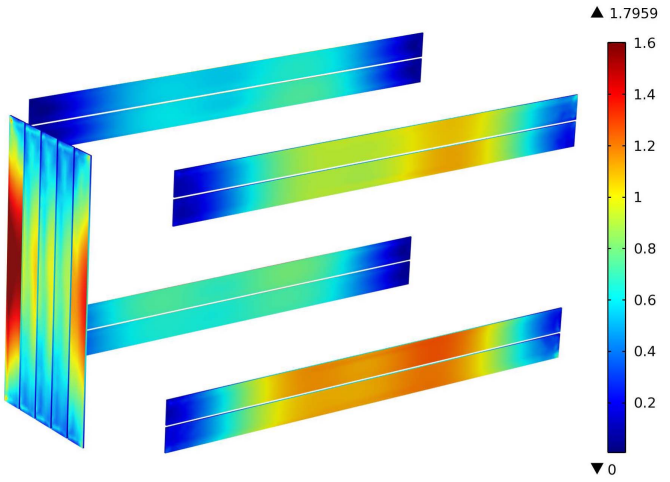


Fig. 11. Magnetic flux distribution (Tesla) in the horizontal and vertical magnetic shunts.

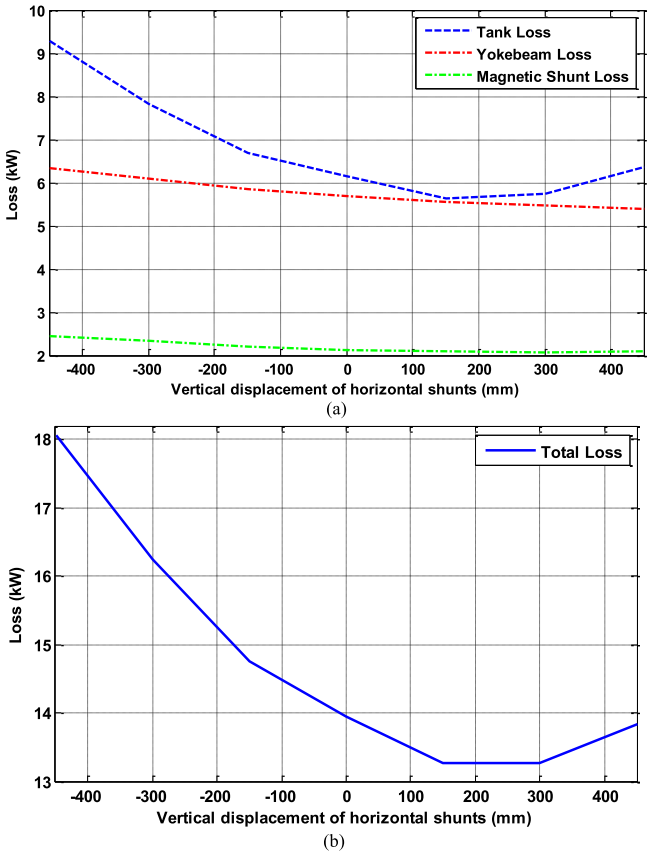


Fig. 12. Parametric FEA results on the vertical position of horizontal shunts. (a) Losses in tank walls, yoke beams, and magnetic shunts. (b) Total losses.

magnetic shunts, and as a result, the total eddy-current losses in the tank walls and the yoke beams are reduced by 83.01% compared with the transformer without wall shunts. Based on Table I, it can be seen that by using the horizontal shunts the total weight of the shunts is reduced by 25% when compared with the vertical shunts while stray losses are almost the same. Thus using horizontal shunt walls would be very cost effective. The magnetic flux distribution in the horizontal and vertical magnetic shunts is shown in Fig. 11. Comparing Figs. 8 and 11 it can be concluded that the flux density in the horizontal arrangements of shunts is higher than vertical arrangements and as a result, the loss density in the horizontal shunts will be higher. Also, it can be seen in Table I that although the total shunt weight with the horizontal shunts is 25% lower compared with the vertical shunts, the shunt losses is 28.5% higher.

Also, parametric FEA was carried out to find the optimal position of the horizontal magnetic shunts for maximum performance. In Fig. 12, the losses versus the gap between yoke beams and the horizontal magnetic shunts are presented. Fig. 12 shows that with 150 mm overlap of the horizontal shunts and yoke beams, the transformer will have the minimum stray losses.

## V. Conclusion

A new method for magnetic shielding of the tank walls in large power transformers has been proposed in this paper. The presented method is based on a horizontal arrangement of magnetic shunts on tank walls. It is shown that the horizontal shunts are as effective as the vertical shunts in reducing stray load losses. However, the horizontal shunts weigh 25% less than the vertical shunts. Hence, the proposed horizontal magnetic shunts arrangement is very cost effective. The proposed combined FEM and analytical method provides an effective and accurate method for the calculation of induced current densities and corresponding eddy-current losses in magnetic wall shunts. It is shown that the flux is not uniformly distributed in the shunt packets; it is higher in the side packets. Also, wall shunt packets in front of the center limb have lower flux densities. Consequently, the thickness of these shunts can be reduced. Furthermore, parametric FEA can be used to find the optimal placement of the magnetic shunts on the tank walls.

## Acknowledgment

This work was supported by the National Science Foundation under Grant CRISP-1541108.

## References

[1] S. V. Kulkarni and S. Khaparde, *Transformer Engineering: Design and Practice*, vol. 25. Boca Raton, FL, USA: CRC, 2004.
[2] R. M. Del Vecchio, B. Poulin, P. T. Feghali, D. M. Shah, and R. Ahuja, *Transformer Design Principles: With Applications to Core-Form Power Transformers*. Boca Raton, FL, USA: CRC, 2010.
[3] K. Karsai and D. Kerényi, and L. Kiss, *Large Power Transformers*. New York, NY, USA: Elsevier, 1987.
[4] Z. Zhu, D. Xie, G. Wang, Y. Zhang, and X. Yan, "Computation of 3-D magnetic leakage field and stray losses in large power transformer," *IEEE Trans. Magn.*, vol. 48, no. 2, pp. 739–742, Feb. 2012.
[5] J. Smajic, G. D. Pino, C. Stemmler, W. Mönig, and M. Carlen, "Numerical study of the core saturation influence on the winding losses of traction transformers," *IEEE Trans. Magn.*, vol. 51, no. 3, pp. 1–4, Mar. 2015.
[6] B. Bai, Z. Chen, and D. Chen, "DC bias elimination and integrated magnetic technology in power transformer," *IEEE Trans. Magn.*, vol. 51, no. 11, pp. 1–4, Nov. 2015.
[7] L. Li, S. Niu, S. L. Ho, W. N. Fu, and Y. Li, "A novel approach to investigate the hot-spot temperature rise in power transformers," *IEEE Trans. Magn.*, vol. 51, no. 3, pp. 1–4, Mar. 2015.
[8] O. Biro, G. Koczka, G. Leber, K. Preis, and B. Wagner, "Finite element analysis of three-phase three-limb power transformers under dc bias," *IEEE Trans. Magn.*, vol. 50, no. 2, pp. 565–568, Feb. 2014.

[9] C. Liao, J. Ruan, C. Liu, W. Wen, and Z. Du, "3-D coupled electromagnetic-fluid-thermal analysis of oil-immersed triangular wound core transformer," *IEEE Trans. Magn.*, vol. 50, no. 11, pp. 1–4, Nov. 2014.

[10] D. Albertz and G. Henneberger, "Calculation of 3D eddy current fields using both electric and magnetic vector potential in conducting regions," *IEEE Trans. Magn.*, vol. 34, no. 5, pp. 2644–2647, Sep. 1998.

[11] J. Olivares, R. Escarela-Perez, S. Kulkarni, F. de Leon, and M. Venegas-Vega, "2d finite-element determination of tank wall losses in pad-mounted transformers," *Electr. Power Syst. Res.*, vol. 71, no. 2, pp. 179–185, 2004. [Online]. Available: http://www.sciencedirect.com/science/article/pii/S0378779604000410

[12] C. Carpenter, "A network approach to the numerical solution of Eddy-current problems," *IEEE Trans. Magn.*, vol. 11, no. 5, pp. 1517–1522, Sep. 1975.

[13] G. Paoli, O. Biro, and G. Buchgraber, "Complex representation in nonlinear time harmonic eddy current problems," *IEEE Trans. Magn.*, vol. 34, no. 5, pp. 2625–2628, Sep. 1998.

[14] M. Moghaddami, A. Moghadasi, and A. I. Sarwat, "An algorithm for fast calculation of short circuit forces in high current busbars of electric arc furnace transformers based on method of images," *Electric Power Syst. Res.*, vol. 136, pp. 173–180, 2016. [Online]. Available: http://www.sciencedirect.com/science/article/pii/S0378779616300037

[15] A. Basak and H. Kendall, "Leakage flux in the steel tank of a 2.5-kVA single phase transformer," *IEEE Trans. Magn.*, vol. 23, no. 5, pp. 3831–3835, Sep. 1987.

[16] L. Li, W. N. Fu, S. L. Ho, S. Niu, and Y. Li, "Numerical analysis and optimization of lobe-type magnetic shielding in a 334 MVA single-phase auto-transformer," *IEEE Trans. Magn.*, vol. 50, no. 11, pp. 1–4, Nov. 2014.

[17] C. Hernandez, M. A. Arjona, and J. P. Sturgess, "Optimal placement of a wall-tank magnetic shunt in a transformer using fe models and a stochastic-deterministic approach," in *Proc. 12th Biennial IEEE Conf. Electromagn. Field Comput.*, Apr./May 2006, p. 468.

[18] M. A. Tsili, A. G. Kladas, P. S. Georgilakis, A. T. Souflaris, and D. G. Paparigas, "Geometry optimization of magnetic shunts in power transformers based on a particular hybrid finite-element boundary-element model and sensitivity analysis," *IEEE Trans. Magn.*, vol. 41, no. 5, pp. 1776–1779, May 2005.

[19] C. Yongbin, Y. Junyou, Y. Hainian, and T. Renyuan, "Study on eddy current losses and shielding measures in large power transformers," *IEEE Trans. Magn.*, vol. 30, no. 5, pp. 3068–3071, Sep. 1994.

[20] M. Djurovic and J. Monson, "3-dimensional computation of the effect of the horizontal magnetic shunt on transformer leakage fields," *IEEE Trans. Magn.*, vol. 13, no. 5, pp. 1137–1139, Sep. 1977.

[21] M. Djurovic and J. E. Monson, "Stray losses in the step of a transformer yoke with a horizontal magnetic shunt," *IEEE Trans. Power App. Syst.*, vol. PAS-101, no. 8, pp. 2995–3000, Aug. 1982.

[22] A. D. Pasquale, G. Antonini, and A. Orlandi, "Shielding effectiveness for a three-phase transformer at various harmonic frequencies," *IET Sci., Meas. Technol.*, vol. 3, no. 2, pp. 175–183, Mar. 2009.

[23] Z. Song *et al.*, "Tank losses and magnetic shunts in a three phase power transformer," in *Proc. Int. Conf. Elect. Mach. Syst. (ICEMS)*, Aug. 2011, pp. 1–4.

[24] F. Dughiero and M. Forzan, "Transient magnetic fem analysis for the prediction of electrodynamic forces in transformers with magnetic shunts," in *IEEE Int. Magn. Conf. (INTERMAG Europe) Dig. Tech. Papers*, Apr. 2002, p. EV5.

[25] Z. Song *et al.*, "The edge effects of magnetic shunts for a transformer tank," in *Proc. Int. Conf. Elect. Mach. Syst. (ICEMS)*, Aug. 2011, pp. 1–4.

[26] H. Kaimori, A. Kameari, and K. Fujiwara, "FEM computation of magnetic field and iron loss in laminated iron core using homogenization method," *IEEE Trans. Magn.*, vol. 43, no. 4, pp. 1405–1408, Apr. 2007.

[27] L. Krahenbuhl, P. Dular, T. Zeidan, and F. Buret, "Homogenization of lamination stacks in linear magnetodynamics," *IEEE Trans. Magn.*, vol. 40, no. 2, pp. 912–915, Mar. 2004.

[28] I. Sebestyen, S. Gyimothy, J. Pavo, and O. Biro, "Calculation of losses in laminated ferromagnetic materials," *IEEE Trans. Magn.*, vol. 40, no. 2, pp. 924–927, Mar. 2004.

[29] J. Gyselinck, L. Vandevelde, J. Melkebeek, P. Dular, F. Henrotte, and W. Legros, "Calculation of eddy currents and associated losses in electrical steel laminations," *IEEE Trans. Magn.*, vol. 35, no. 3, pp. 1191–1194, May 1999.

[30] A. G. Jack and B. C. Mecrow, "Calculation of three-dimensional electromagnetic fields involving laminar eddy currents," *IEE Proc. A, Phys. Sci., Meas. Instrum., Manage. Edu.-Rev.*, vol. 134, no. 8, pp. 663–671, Sep. 1987.

[31] K. Preis, O. Biro, and I. Ticar, "FEM analysis of eddy current losses in nonlinear laminated iron cores," *IEEE Trans. Magn.*, vol. 41, no. 5, pp. 1412–1415, May 2005.

[32] R. F. Hemmings and G. D. Wale, "Heating in transformer cores due to radial leakage flux. Part 1: Experimental models and test results," *Proc. Elect. Eng. Inst.*, vol. 124, no. 11, pp. 1064–1072, Nov. 1977.

[33] C. J. Carpenter, K. O. Sharples, and M. Djurovič, "Heating in transformer cores due to radial leakage flux. Part 2: Computed results," *Proc. Elect. Eng. Inst.*, vol. 125, no. 11, pp. 1265–1268, Nov. 1978.

[34] C. J. Carpenter, "Theory of flux penetration into laminated iron and associated losses," *Proc. Elect. Eng. Inst.*, vol. 124, no. 7, pp. 659–664, Jul. 1977.

[35] C. J. Carpenter and M. Djurovi, "Three-dimensional numerical solution of eddy currents in thin plates," *Proc. Elect. Eng. Inst.*, vol. 122, no. 6, pp. 681–688, Jun. 1975.

[36] V. C. Silva, G. Meunier, and A. Foggia, "A 3-D finite-element computation of eddy currents and losses in laminated iron cores allowing for electric and magnetic anisotropy," *IEEE Trans. Magn.*, vol. 31, no. 3, pp. 2139–2141, May 1995.